








# A Search for Gravitationally Lensed Gamma-Ray Bursts in the Data of the Interplanetary Network and *Konus-Wind*

K. Hurley<sup>1</sup> , A. E. Tsvetkova<sup>2</sup> , D. S. Svinkin<sup>2</sup> , R. L. Aptekar<sup>2</sup>, D. D. Frederiks<sup>2</sup> , S. V. Golenetskii<sup>2</sup>, A. A. Kokomov<sup>2</sup>, A. V. Kozlova<sup>2</sup>, A. L. Lysenko<sup>2</sup> , M. V. Ulanov<sup>2</sup>, T. L. Cline<sup>3</sup>, I. G. Mitrofanov<sup>4</sup>, D. Golovin<sup>4</sup>, M. L. Litvak<sup>4</sup>, A. B. Sanin<sup>4</sup>, W. Boynton<sup>5</sup>, K. Harshman<sup>5</sup>, C. Fellows<sup>5</sup>, R. Starr<sup>6</sup>, A. Rau<sup>7</sup>, A. von Kienlin<sup>7</sup>, and X. Zhang<sup>7</sup>

<sup>1</sup> University of California, Berkeley, [khurley@ssl.berkeley.edu](mailto:khurley@ssl.berkeley.edu)

<sup>2</sup> Ioffe Institute, Politeknicheskaya 26, St. Petersburg 194021, Russia

<sup>3</sup> NASA Goddard Space Flight Center, Greenbelt, MD 20771, USA<sup>8</sup>

<sup>4</sup> Space Research Institute of the Russian Academy of Sciences, Moscow 117997, Russia

<sup>5</sup> Lunar and Planetary Laboratory, University of Arizona, Tucson, AZ 85719, USA

<sup>6</sup> Catholic University of America, Washington, DC 20064, USA

<sup>7</sup> Max-Planck-Institut für extraterrestrische Physik, Giessenbachstrasse, Postfach 1312, Garching, D-85748 Germany

Received 2018 August 31; revised 2018 November 30; accepted 2018 December 3; published 2019 January 25

## Abstract

We examine a sample of 2301 gamma-ray bursts, detected by *Konus-Wind* in the triggered mode between 1994 and 2017 and localized by the interplanetary network (IPN), for evidence of gravitational lensing. We utilize all the available gamma-ray burst (GRB) data: time histories, localizations, and energy spectra. We employ common IPN techniques to find and quantify similarities in the light curves of 2,646,150 burst pairs, and for the pairs with significant similarities, we examine their IPN localizations to determine whether they are consistent with a common origin. For pairs that are consistent, we derive and compare energy spectra, and compute a figure of merit that allows us to compare and rank burst pairs. We conduct both a blind search, between all possible burst pairs, and a targeted search, between pairs in which one burst has both a spectroscopic redshift and an identification of an intervening system, as measured by one or more lower spectroscopic redshifts. We identify six pairs in the blind search that could be taken as evidence for lensing, but none are compelling enough to claim a detection with good confidence. No candidates were detected in the targeted search. For our GRB sample, we set an upper limit to the optical depth to lensing of 0.0033, which is comparable to that of optical sources. We conclude that proposed scenarios in which a large fraction of the GRB population is lensed are extremely unlikely.

*Key words:* gamma-ray burst; general – gravitational lensing; strong

## 1. Introduction

The spectroscopically measured redshifts of cosmic gamma-ray bursts (GRBs) span the range from 0.0085 (Tinney et al. 1998) to 6.29 (Kawai et al. 2005), and even more distant redshifts have been measured photometrically (e.g., Cucchiara et al. 2011). The redshifts of gravitationally lensed optical sources range from 0.102 to 5.699 (Kochanek et al. 2018). If we assume that the optical depth to lensing is identical for the two types of sources, the probability that a GRB at redshift greater than 1 is strongly gravitationally lensed may be in the range  $10^{-2}$ – $10^{-4}$  (Turner et al. 1984; Treu 2010). An independent estimate puts the probability of GRB lensing at up to 60% (Wyithe et al. 2011). This implies that in a sample of several thousand bursts, we might expect several lensed sources, and possibly many more. Indeed, a search through the Gamma-Ray Burst Coordinates Network Circulars<sup>9</sup> reveals that over 50 bursts display intervening redshifts in addition to source redshifts, suggesting that the bursts are candidates for lensing. One of the broader consequences of the existence of lensed bursts is that, whether or not they are identified as such, they may be significantly magnified to apparently very high luminosities (or reduced to lower ones, Petitjean et al. 2016 and references therein) with implications for studies involving their apparent luminosities and beaming angles. A good example in the optical is the apparently superluminous supernova PS1-10afx,

whose observed flux is roughly 30 times too bright compared to templates, but which can be explained by magnification by a gravitational lens (Quimby et al. 2013). Indeed, Wyithe et al. (2011) have estimated GRB magnifications of up to 50. But whereas optical lensing is identified primarily by sources with separations of arcseconds, often in conjunction with measurements of source and lens redshifts, and/or inferred time delays, of the over 700 GRBs with optical counterparts, the number with spectroscopically measured redshifts is less than 500, and none of them lie within arcseconds of one another. Thus an effective search for gravitationally lensed bursts requires a different strategy.

If we consider all the observed GRBs, regardless of whether their counterparts have been identified, we have a data set with numerous advantages over optical sources. There are no observing seasons, cadence, or campaign length considerations. Their distribution is isotropic. Triggered GRBs announce themselves, so no searches for them are required. The data span several decades, so very long delays can in principle be found. Burst light curves generally have high signal-to-noise ratios, and the majority are not truncated and do not have data gaps. The time delay between a pair of bursts can be measured very accurately, to tens of milliseconds in the best cases. Finally, in contrast to the optical situation, the intervening galaxy has no absorbing effect on the GRB light curves. However, the data set has drawbacks too. Proof of lensing would ideally require identical time histories, nearly identical precise localizations, and measurements of both the source and intervening system

<sup>8</sup> Emeritus.

<sup>9</sup> <https://gcn.gsfc.nasa.gov/gcn/>

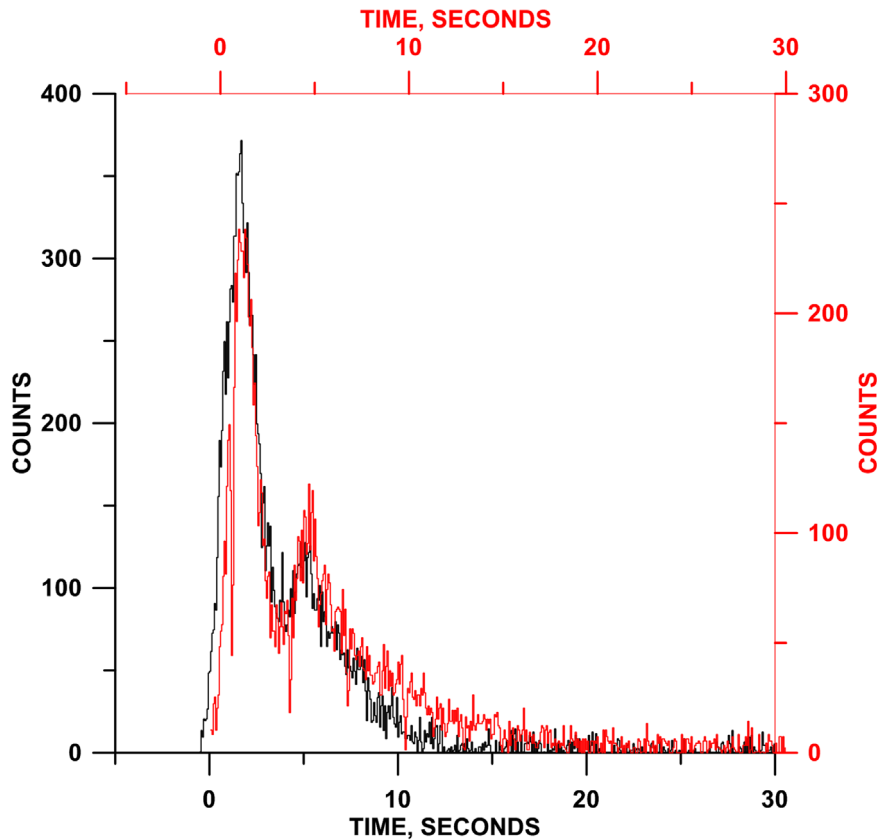


**Figure 1.** Background-subtracted *Konus* time histories of GRB 090406 (black) and 130320 (red), aligned for the time lag with the maximum correlation coefficient (0.96). GRB 130320 starts nine time intervals (0.576 s) after GRB 090406 in this alignment. For clarity, only the first 30 s after trigger are shown. Although the time histories are similar, the localizations of the two bursts are inconsistent with one another.

redshifts. Identical energy spectra would also be expected. However, the weaker component of a lensed, strongly magnified burst might not trigger a detector, or if it does, its time history might not contain all the features that the stronger component has. Also, because GRBs are compact sources, microlensing may be present in lensed sources, which can alter the time history of the lensed burst and make comparisons of light curves difficult. Similarly, energy spectra may differ if the lensed and direct parts of a jet are observed. In addition, although the redshift distribution of bursts is known, the redshifts of most bursts have not been measured. Finally, many bursts are poorly localized, to tens of square degrees, making it difficult to establish whether they originate from the same source.

In this paper we present a study of 2301 GRBs that occurred between 1994 and 2017, whose time histories and energy spectra were measured by *Konus-Wind* in the triggered mode, and many of which were localized by the interplanetary network (IPN). In the following section, we discuss how this sample was obtained and point out some of its unique features. Then we explain the method used for comparing time histories and determining whether bursts have localizations that would be consistent with a common origin. We also discuss energy spectra comparisons. Finally we present our results and discuss their interpretation.

## 2. The GRB Sample

The *Konus-Wind* (Aptekar et al. 1995) triggered GRB data have several unique features that make them ideal for this

study. First, the spacecraft is in interplanetary space at distances up to 7 lt-s from Earth, which means that the background is steady and there is no Earth-blocking or Earth albedo. Second, the duty cycle  $d$  is  $\sim 95\%$ . Third, the entire sky is covered by two cylindrically symmetrical, omnidirectional detectors whose axes are aligned with the spacecraft spin axis and always point toward the north and south ecliptic poles. Finally, the constant orientation of the axes means that two bursts coming from the same direction, but at different times, would always arrive at the detectors at the same angle to the axis, minimizing systematic response differences. The weakest triggered burst with a measured fluence had  $7 \times 10^{-8}$  erg  $\text{cm}^{-2}$ , 15–150 keV (these are typically the very shortest bursts). The weakest triggered burst with a measured 1 s peak flux had 0.7 photons  $\text{cm}^{-2} \text{s}^{-1}$ , 15–150 keV. Descriptions of the trigger algorithm may be found in Svinkin et al. (2016) and Tsvetkova et al. (2017). The redshifts of 133 triggered *Konus* bursts have been measured spectroscopically; they range from 0.125 to 5. We began by defining an initial sample of 2812 triggered bursts between 1994 November 17 (the first event detected) and 2017 March 30 (the cutoff date for this study); this sample eliminates events classified as solar, soft gamma repeater, or particle, and includes only GRBs. Although it would have been possible to include many more bursts in the initial sample if we considered other instruments in addition to *Konus-Wind*, we chose to avoid the systematics of light-curve comparisons between different detectors. Similarly, other databases (e.g., BATSE, *Fermi*) contain more light curves, but Earth-blocking, duty cycle, and background variations present significant disadvantages. We utilized the 64 ms resolution *Konus* light curves, which contain

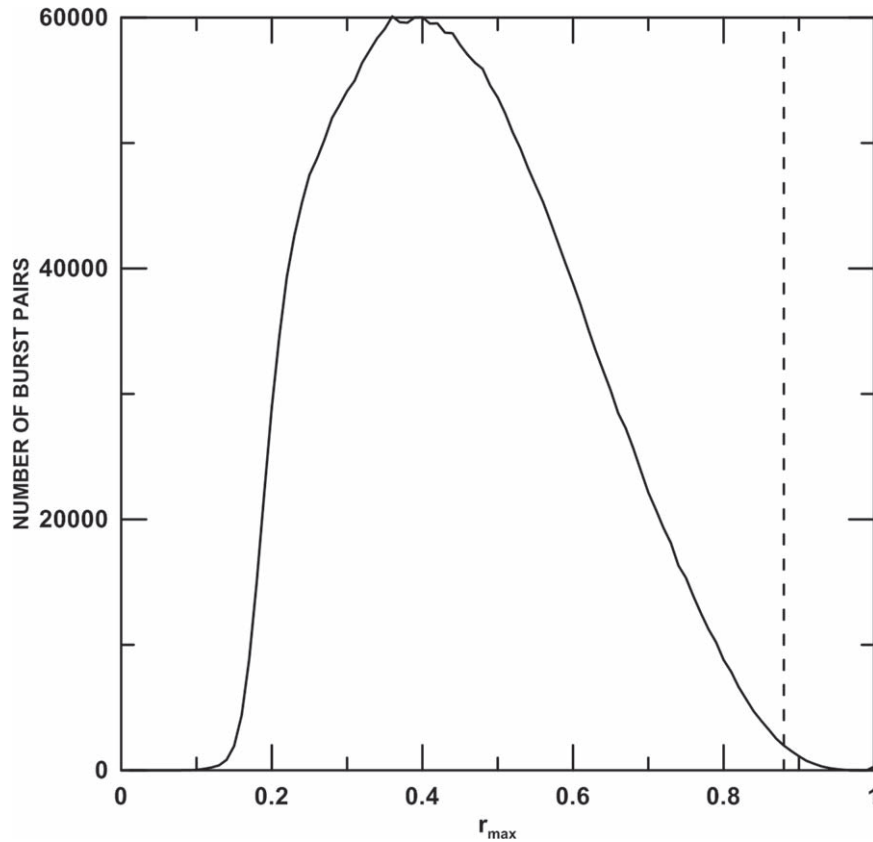


**Figure 2.** The distribution of the values of the maximum correlation coefficient  $r_{\max}$  for 2,646,150 GRB pairs. 6523 pairs, or 0.25%, have  $r_{\max} > 0.88$  (dashed vertical line).

99.26 s of data; these light curves are publicly available.<sup>10</sup> By visual examination, we eliminated the following. First, very short duration bursts, ( $< 2$  s), whose time histories are relatively featureless; our light-curve comparison method (see below) identifies pairs of such bursts as strongly resembling one another, but the resemblance is not significant. We refer to this as the duration criterion. And second, burst time histories with data gaps, noise, or truncated data that could not be repaired and would alter the light curve. 2301 bursts remained after this selection process; we refer to them as “the sample.” The acceptance rate  $a$  is therefore  $2301/2812$ , or 0.82.

No selection is made based on the time delays between burst pairs. However, once *Konus-Wind* has triggered on a burst, it cannot retrigger for 3621 s; in principle, bursts occurring within this time window can be found in the spacecraft housekeeping data (80–360 keV, 3.68 s time resolution, 256 count resolution due to scaling), but this search does not utilize those data, so it is insensitive to time delays in this range. To estimate the effect on this study, the IPN master list<sup>11</sup> was searched for bursts following *Konus* triggers in the sample by less than 3621 s, as recorded by any spacecraft in the network. 41 bursts were found (a rate of 1.8 per year), leading to a probability estimate of 0.0178 that a burst pair could be missed. Between 1994 and 2017, there were periods when instruments with greater sensitivity than *Konus* were operating, namely BATSE (1994–2000) and *Fermi* GBM (2008–2017). During these periods, the search would have identified bursts below the *Konus* threshold, which would increase the number of events.

However, between 2000 and 2008, IPN instruments with less sensitivity were in the network, which would decrease the number and tend to compensate for this. We have repeated the analysis by searching for events following BATSE and *Fermi* bursts. After correcting for sky coverage and duty cycle, rates of 5.5 and 10.9 per year were found. However, these higher rates are most likely due simply to the greater sensitivities of these two instruments, and it would not be possible to adjust them to the *Konus* trigger threshold due to the very different triggering algorithms for the three experiments. Thus we believe that the search with *Konus* triggers produces the most accurate result, and we take the time delay sensitivity  $s$  to be 1–0.0178 or 0.982.

### 3. Light-curve Comparisons

To identify candidate lensed burst pairs, we compared the light curve of each burst in the sample with every other burst; this resulted in 2,646,150 such comparisons. Light-curve comparisons are an integral part of the interplanetary network methodology; comparisons between different detectors recording the time history of the same GRB establish a time delay that is used to generate a localization annulus. The light curves of these bursts are intrinsically identical, and the observed light curves are nearly so when differences in detectors are taken into account. Over 10,000 such comparisons have been done, and numerous cross-checks and calibrations (e.g., triangulations of bursts whose locations are precisely known from their counterparts) have been carried out to refine and confirm the methods used. Both the correlation coefficient and a chi-squared analysis are employed, the latter mainly to estimate the

<sup>10</sup> [https://gen.gsfc.nasa.gov/konus\\_grbs.html](https://gen.gsfc.nasa.gov/konus_grbs.html)

<sup>11</sup> <http://www.ssl.berkeley.edu/ipn3/masterli.txt>

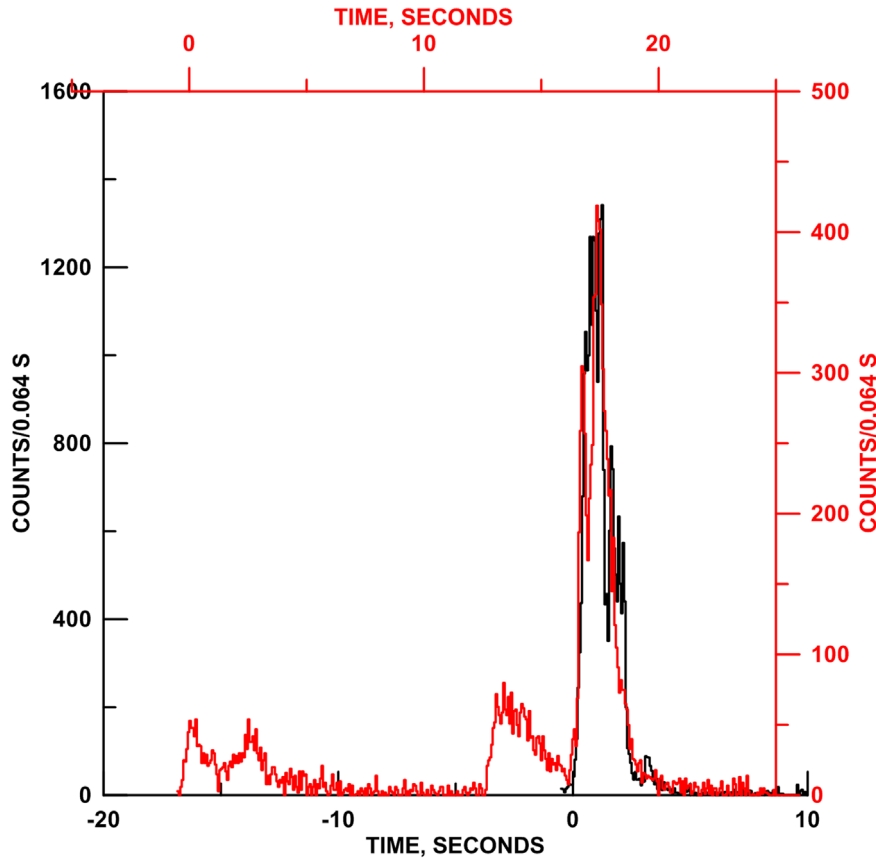


**Figure 3.** Background-subtracted light curves for GRB 060315 (black) and 160829 (red). The time histories are aligned for  $r_{\max} = 0.933$ , which is well above the 0.88 threshold, and the bursts have localizations consistent with a common origin. However, three peaks in GRB 160829 occur before the trigger time in 060315, and 119 time intervals in 160829 exceeded the trigger threshold for 060315. Extreme microlensing would have to be invoked for the light curve of 160829 to explain this, and this burst pair is rejected.

confidence limits for the time delays, which determine the width of the triangulation annulus. Here, however, we are interested only in rejecting burst pairs with time histories that do not resemble one another, and identifying those which do, while allowing for reasonable differences due to magnification and/or microlensing. The confidence limits for time delays are unimportant for lensed bursts, because they are negligibly small compared to the delays themselves. Thus we utilize only the correlation coefficient to establish the degree of similarity of a time history pair.

We start with the raw light curves of two different bursts. We estimate the background by selecting the last 20 time intervals in the light curve, which generally display no burst activity. Outliers were flagged and examined visually to select a new background interval. We subtract the background from each to form light curves, which we will call  $x_i$ ,  $y_j$ .  $x$  and  $y$  are in counts, and  $i$  and  $j$  identify the time intervals. We calculate the average number of counts  $\bar{x}$ ,  $\bar{y}$ , and the standard deviations  $s_x$ ,  $s_y$ . The definition of the correlation coefficient is

$$r(t) = \sum(x_i - \bar{x})(y_j - \bar{y}) / (s_x s_y n),$$

where  $t$  is the time lag between the two light curves. The sum is over the  $n$  time bins that  $x_i$  and  $y_j$  have in common for the lag  $t$ .  $r(t)$  can vary between  $-1$  and  $+1$  by definition; higher values are indicative of a stronger correlation. Note that  $r(t)$  is insensitive to changes in the light curves by a multiplicative factor. This means that a pair of light curves has the same  $r(t)$  regardless of whether one light curve is magnified.

The lag is allowed to vary, but a minimum of 10 s of overlap between the light curves is required for good statistics; that is, at the maximum lag between  $x_i$  and  $y_j$ , the first light curve  $x_i$  must start a minimum of 10 s before the end of the second one  $y_j$ , and the lag is decreased until the start of the second light curve  $y_j$  is positioned a minimum of 10 s before the end of the first one  $x_i$ . The maximum value of the correlation coefficient  $r_{\max}$  and the lag for which it occurred are recorded. An example is shown in Figure 1. In Figure 2 we present the distribution of 2,646,150 values of  $r_{\max}$ . 6523 GRB pairs, or 0.25%, have  $r_{\max} > 0.88$ , so we define this as an empirical, approximately  $3\sigma$  equivalent value, below which the correlation is likely to be statistically insignificant. The localizations of burst pairs above this value are examined to see whether they are consistent with a common arrival direction. Note that a given event may occur in more than one of the 6523 pairs, which could, in principle, be taken as evidence for multiple images.

Even if  $r_{\max} > 0.88$  for a burst pair, however, it may not be a good candidate for a lensed pair. This is illustrated in Figure 3, which shows two bursts, GRB 060315 and GRB 160829, with  $r_{\max} = 0.933$ , but which have features missing from one light curve prior to its trigger. To determine whether this could occur by chance, we calculate the approximate trigger thresholds for each candidate burst pair and ask whether the light curve of the event with the missing features (GRB 060315 in this case) could have triggered late by chance. We refer to this as the trigger criterion. For this particular pair, 119 time intervals in GRB 160829 were above the trigger threshold for 060315,

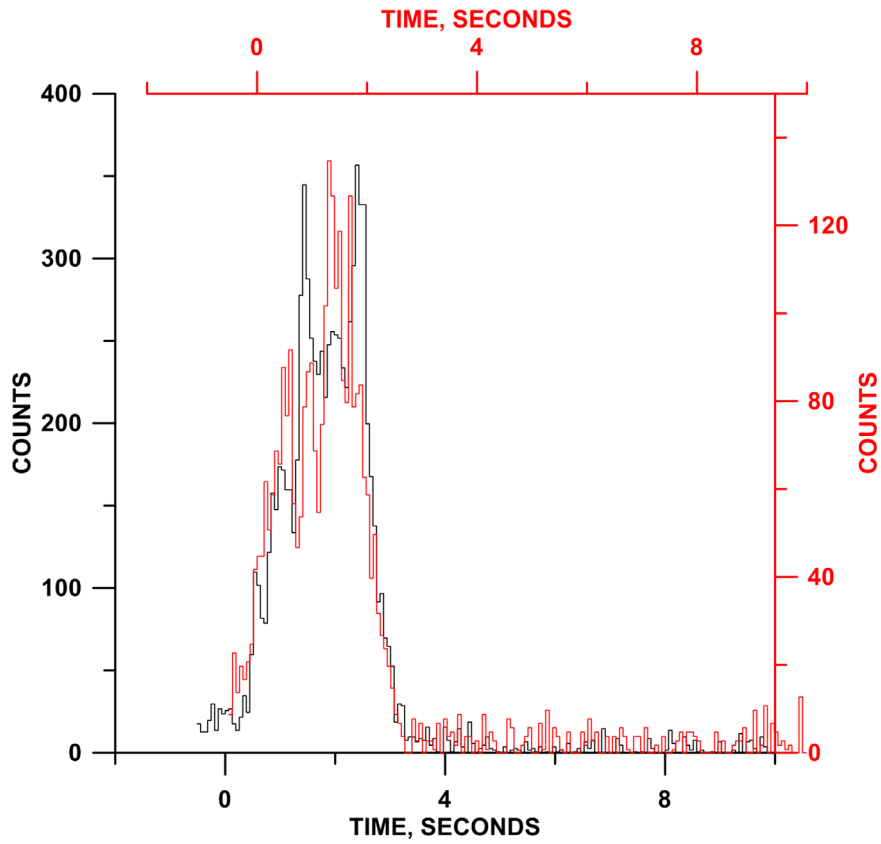


**Figure 4.** Background-subtracted *Konus* time histories of GRB 950704 (black) and 051012 (red), aligned for the time lag with the maximum correlation coefficient (0.910). Numerous features of the two events do not correspond. Statistical fluctuations and microlensing would have to be invoked to explain this.

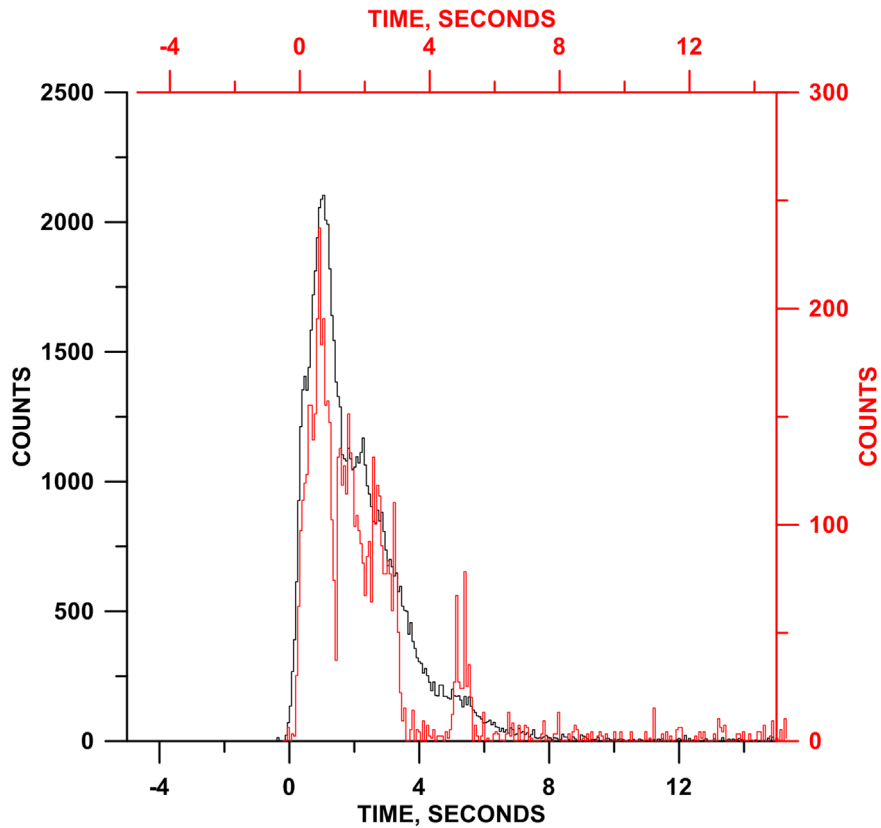


**Figure 5.** Background-subtracted *Konus* time histories of GRB 960924 (black) and 020303 (red), aligned for the time lag with the maximum correlation coefficient (0.939). Numerous features in the weaker event (020303) are missing from the stronger one (960924), and the stronger burst is approximately 10 times more intense. Both strong magnification and microlensing would have to be invoked to explain this.

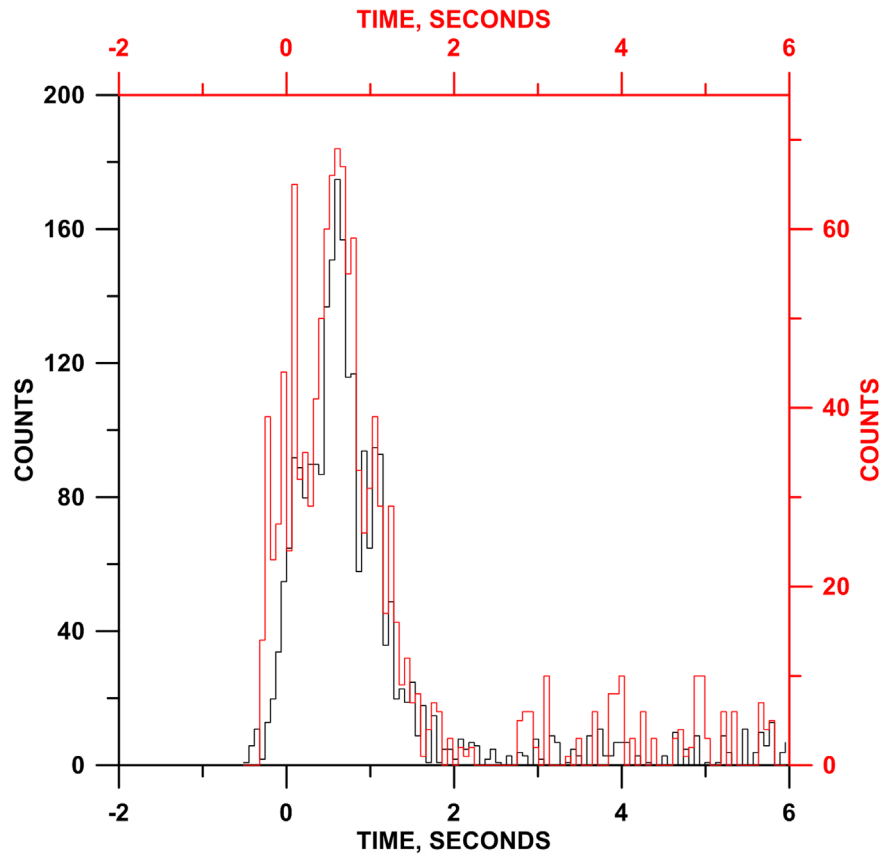


**Figure 6.** Background-subtracted *Konus* time histories of GRB 000821 (black) and 041007 (red), aligned for the time lag with the maximum correlation coefficient (0.891). Given the weak statistics, the agreement is reasonable.

making this possibility extremely unlikely. An approximate upper limit to the probability may be calculated as follows. Assume that a light curve has  $N$  time intervals with average count rates just at the trigger level. Then the probability that any time interval would be below the trigger level is 0.5, and the probability that all  $N$  would be below it is  $0.5^N$ . Thus if any time history has more than 10 intervals above the trigger threshold, the probability that it would not trigger is  $<0.00098$ . In practice, we rejected burst pairs with  $N > 10$ ; there were 44 such rejections. This is an upper limit to the probability of not triggering for two reasons. First, in the example of Figure 3, the count rates of GRB 160829 are not at the trigger level, but well above it. Second, *Konus-Wind* has two trigger criteria, based on different time intervals. The only other explanation for a missed trigger would be an extreme case of microlensing, which we do not invoke in this study. In all the cases where a pair was rejected by the trigger criterion, we have examined the light curves in detail using the *Konus* waiting mode data, which provide a continuous record with 2.9 s resolution. In all cases but one, visual analysis and/or signal-to-noise ratio calculations supported the rejection. In only one case, these tests were inconclusive, but that pair had inconsistent localizations as determined by their ecliptic latitudes. We do not reject burst pairs where the post-trigger time histories display slightly different features, as long as they meet the  $r_{\max}$  criterion; examples are given below. Similarly, we do not reject burst pairs based on their relative intensities; weak bursts may precede strong ones, and vice versa, in this study. The rationale is that, although the later burst in a gravitationally lensed pair

may have traveled farther, it may also be magnified to an apparent intensity that is greater than the earlier burst.

Although cosmological time dilation is not explicitly taken into account in these calculations, this method is tolerant to it. The degree of tolerance depends on the time history. To test this, the single-peaked time history of GRB 000821 (Figure 6), which has moderately good statistics, was stretched by factors of up to 1.6, and cross-correlated with its undilated version. The  $r_{\max} > 0.88$  criterion was satisfied. A more complex time history, such as that of GRB 990123 (discussed in Section 6, but not shown), which has very good statistics and multiple peaks, tolerates only about a factor of 1.15. This tolerance also extends to gravitational time dilation in the case where one path passes closer to a massive black hole.

#### 4. Localization and Energy Spectra Comparisons

If a burst pair meets the  $r_{\max}$  criterion, we obtain the probability  $P_1$  of a correlation coefficient this large or larger from the distribution of Figure 2, and examine the localizations of the bursts to see if they are consistent with a common origin. The IPN website<sup>12</sup> contains localization information for over 7700 bursts. The majority have been localized by triangulation, which results in one or more triangulation annuli. Additional localization information has been added where appropriate. This includes, but is not limited to, BATSE, *Fermi* GBM, *Swift*, INTEGRAL-IBIS, and *BeppoSAX* error circles, as well as ecliptic latitude constraints derived from the *Konus-Wind* data, and planet-blocking information for spacecraft in low

<sup>12</sup> <http://www.ssl.berkeley.edu/ipn3/index.html>

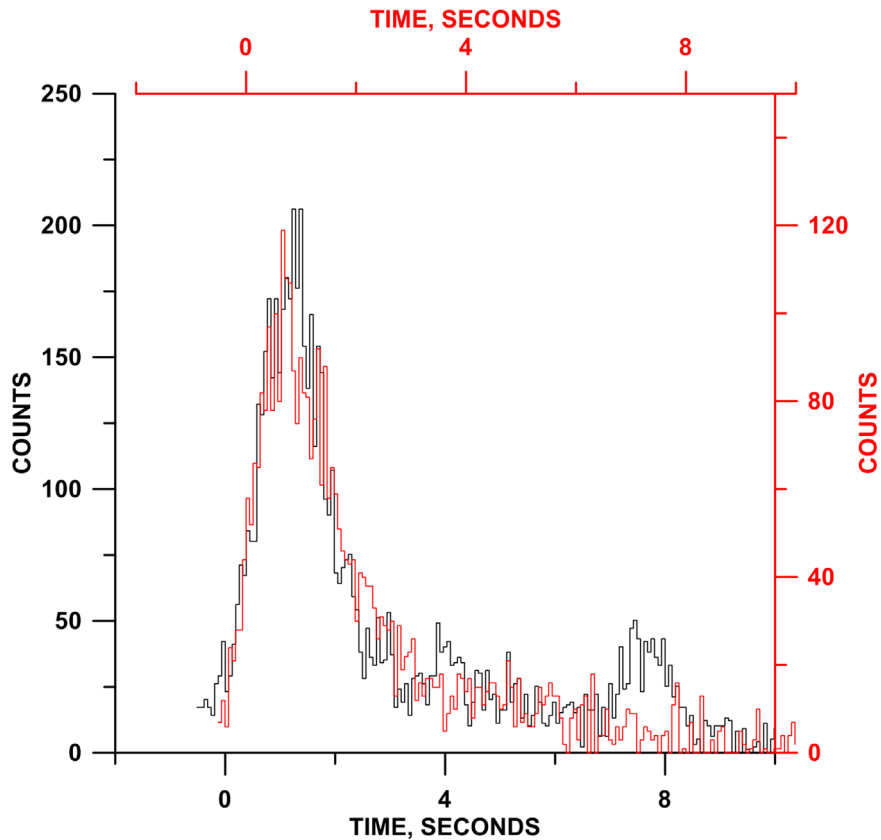


**Figure 7.** Background-subtracted *Konus* time histories of GRB 950114 (black) and 151021 (red), aligned for the time lag with the maximum correlation coefficient (0.898). Two features in the light curve of 950114, at 4 and 7 s, do not correspond to 151021. A combination of weak statistics and microlensing would have to be invoked to explain this.

Earth or Mars orbit. A possible common origin means that a region must exist that is consistent with all the localization information for a candidate burst pair. The average probability of random overlap of two localizations in the database is of the order of 0.008 or more. Of the 6523 burst pairs, 51 had localizations consistent with a common origin. Of the 51, 6 met the trigger criterion ( $N \leq 10$ ). We discuss them in the next section.

The IPN localization technique, when combined with planet-blocking, error circles, or ecliptic latitude bands from other spacecraft, can produce a wide variety of error box shapes, ranging from very small, well-defined boxes to complex sections of annuli. Each is unique for a given burst. The probability of a chance intersection of two localizations can range from vanishingly small for two small error boxes, to 1 for two annuli that are composed of great circles. To estimate the probability of a chance overlap of two localization regions for a pair of bursts, simulations were carried out. There are numerous ways to formulate the question; the one used here is the following. Given a fixed localization for the first burst, what is the probability that a second burst, arriving from any point in the sky, has a localization consistent with the first one? To answer this question, the position of the first burst was held constant, while the arrival direction of the second one was varied over a grid of approximately 300 evenly spaced points on the celestial sphere ( $\sim 11.7^\circ$  apart). For each point, the arrival times at the spacecraft were calculated for the second burst, and localization annuli were calculated. The spacecraft positions were held fixed, but other localization information, such as BATSE, GBM, and other error circles, as well as ecliptic

latitude bands, were moved to agree with the simulated arrival direction. Arrival directions which were planet-blocked to the spacecraft of the second burst were skipped. The resulting new localizations of the second burst were compared to that of the first burst, and the number of overlaps was counted to arrive at the probability  $P_2$  of a chance coincidence.

To estimate the significance of matching energy spectra, the Band function (Band et al. 1993) spectral fitting parameters ( $\alpha$ ,  $\beta$ , and  $E_{\text{peak}}$ ) and their uncertainties were extracted for 2132 *Fermi* GBM bursts from the HEASARC.<sup>13</sup> The spectral parameters of all pairs of bursts were compared; this resulted in 2,271,646 comparisons. 115,226 burst pairs had  $\alpha$ ,  $\beta$ , and  $E_{\text{peak}}$ , which agreed to within their uncertainties. Thus an estimate of the probability of a chance spectral match between burst pairs is 0.051, and a spectral match, in conjunction with the time history and localization matches, lends further weight to a gravitational lensing hypothesis. The probability of a mismatch of 1, 2, or all 3 parameters is  $1 - 0.051$ , or 0.949. Burst pairs are not rejected if the spectra do not match; the spectral match or mismatch probability is referred to as  $P_3$ . The *Fermi* spectral archive was chosen for this estimate because there is presently no *Konus* spectral archive. It is possible that the better statistics of GBM spectra will lead to tighter constraints on the Band parameters, and therefore that our estimate of the probability of a spectral match is lower than it would be if the *Konus* data were used.

While consistent localizations are an absolute requirement for a lensed pair, there is more flexibility with the time histories

<sup>13</sup> <https://heasarc.gsfc.nasa.gov/>

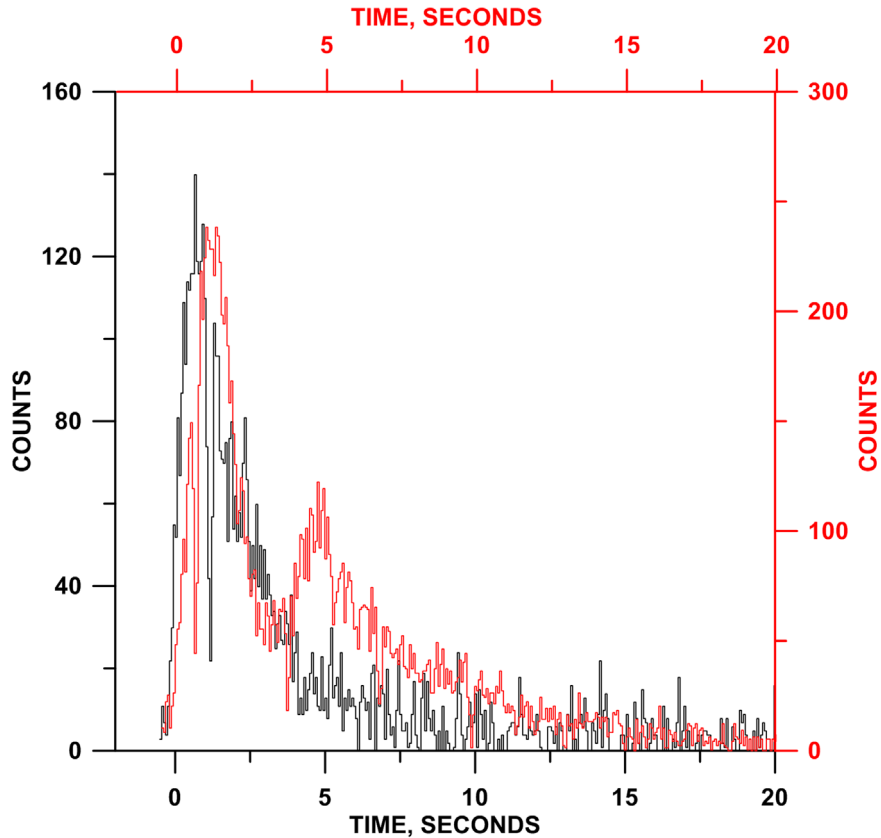


**Figure 8.** Background-subtracted *Konus* time histories of GRB 990312 (black) and 020303 (red), aligned for the time lag with the maximum correlation coefficient (0.891). Numerous features of the two events do not correspond, which could be at least partly explained by occultation from spacecraft structures.

and energy spectra if microlensing and lensing different parts of a jet are allowed. Nevertheless, without assigning different weights to the probabilities, a formal joint probability  $P_j$  can be obtained from the product  $P_1 \times P_2 \times P_3$ , and used as an approximate figure of merit to compare and rank the burst pairs; smaller  $P_j$  indicate smaller chance coincidence probabilities, and therefore higher confidence.

### 5. Candidate Gravitationally Lensed Burst Pairs

The light curves of the six burst pairs that met all the search criteria are shown in Figures 4–9, in order of increasing  $P_j$  and lower confidence. In these figures, the ordinate of one light curve has been adjusted so that the peaks of the two time histories are roughly aligned to facilitate a visual comparison. The abscissa of one light curve has been shifted to show the time delay where  $r$  reaches its maximum. In Figure 10, the localizations of one burst pair are shown as an example. The six pairs involve nine different bursts; three bursts appear in two pairs each, but their localizations exclude a multiply imaged burst. We discuss each pair in detail below, and summarize the results in Table 1, which also indicates the IPN spacecraft that observed each burst. The time-integrated spectral fits, using the Band function (Band et al. 1993) and the *Konus* data, are given in Table 2. The GRB dates are given as year, month, day, and seconds of day.

GRB 19950704\_11431/20051012\_43209. The time delay is 3753 days. The light curves of this pair are shown in Figure 4, aligned for the lag with the largest correlation coefficient (0.910,  $P_1 = 7.2 \times 10^{-4}$ ). GRB 950704 is localized to a long, narrow IPN annulus; GRB 051012 is localized to two sections

of a wide IPN annulus. The probability of a chance overlap between the two is a relatively large  $P_2 = 0.16$ . All spectral parameters agree to within uncertainties, so  $P_3 = 0.051$ ; the later burst has 0.45 times the fluence of the earlier one. Some features in the light curve of 950704 do not appear in 051012, and vice versa, which could be explained by a combination of statistics and microlensing. However, the relatively large probability of a chance overlap makes a lensing explanation uncertain.  $P_j = 5.9 \times 10^{-6}$ .

GRB 19960924\_42119/20020303\_82040. The time delay is 1986 days. The light curves of this pair are shown in Figure 5, aligned for the lag with the largest correlation coefficient (0.939,  $P_1 = 1.2 \times 10^{-4}$ ). GRB 960924 is localized to a BATSE error circle and an IPN annulus; GRB 020303 is localized to an IPN annulus and a wide ecliptic latitude band, and the probability  $P_2$  of a chance overlap between the two is approximately 0.029.  $E_{\text{peak}}$  and  $\beta$  agree within uncertainties for the two spectra, but  $\alpha$  disagree, so  $P_3 = 0.949$ ; the later burst has 0.093 times the fluence of the earlier one. The light curve of 20020303 has strong features that are not present in 19960924, making this an unlikely lensing candidate pair unless strong microlensing is assumed.  $P_j = 3.3 \times 10^{-6}$ .

GRB 20000821\_33589/20041007\_07328. The time delay is 1507 days. The light curves of this pair are shown in Figure 6, aligned for the lag with the largest correlation coefficient (0.891,  $P_1 = 1.1 \times 10^{-3}$ ). GRB 000821 is localized to a section of a narrow IPN annulus; GRB 041007 is localized to a long, narrow IPN error box. The probability of a chance overlap is approximately  $P_2 = 0.02$ . Both bursts are relatively weak, and statistics could explain their differences. However, while the spectral indices  $\alpha$  and  $\beta$  and the fluxes match, the



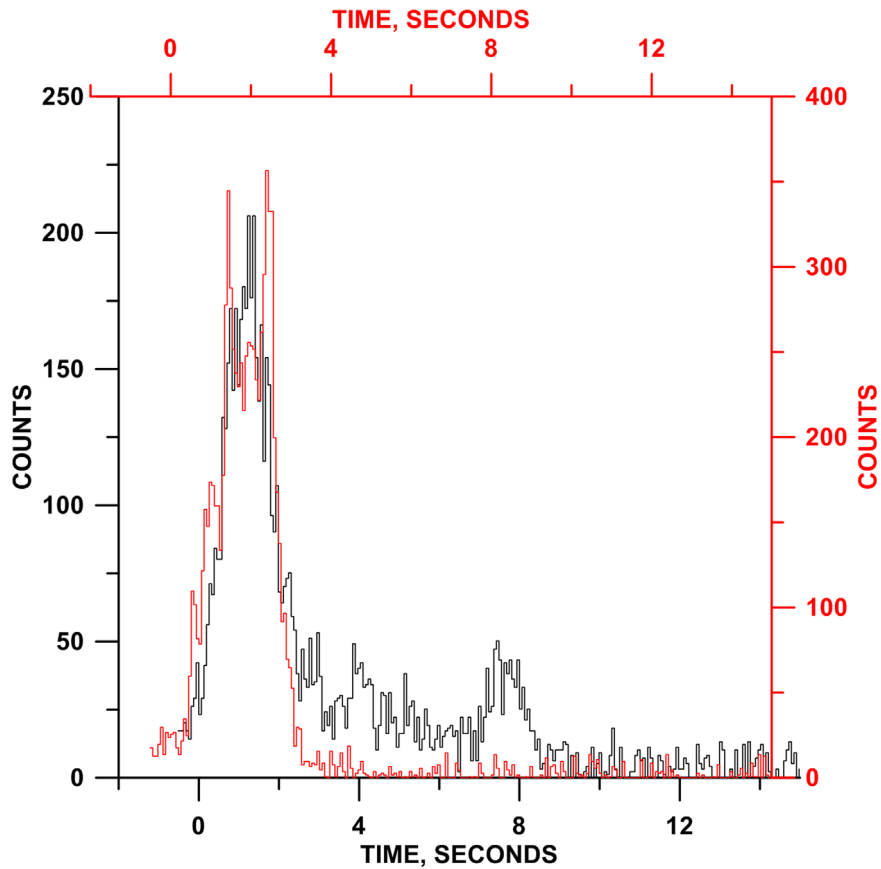


**Figure 9.** Background-subtracted *Konus* time histories of GRB 950114 (black) and 950704 (red), aligned for the time lag with the maximum correlation coefficient (0.883). Microlensing would be required to explain the differences in the two light curves.

peak energies  $E_{\text{peak}}$  differ by a factor of 7.4. The later burst has 1.7 times the fluence of the earlier one.  $P_3 = 0.949$ , and  $P_j = 2.1 \times 10^{-5}$ .

GRB 19950114\_47434/20151021\_68368. The time delay is 7585 days. The light curves of this pair are shown in Figure 7, aligned for the lag with the largest correlation coefficient (0.898,  $P_1 = 1.1 \times 10^{-3}$ ). GRB 950114 is localized to a section of a narrow IPN annulus; 151021 is localized to an IPN error box and a *Fermi* GBM error circle. The probability of a chance overlap is approximately  $P_2 = 0.023$ . The spectral indices  $\alpha$  and  $\beta$  and the fluxes of this pair match, but  $E_{\text{peak}}$  for 950114 is about half that of 151021, so  $P_3 = 0.949$ . The later burst has 1.1 times the fluence of the earlier one. A combination of microlensing and weak statistics could plausibly account for this candidate pair. Figure 10 shows the localizations for this pair.  $P_j = 2.4 \times 10^{-5}$ .

GRB 19990312\_69909/20020303\_82040. The time delay is 1087 days. The light curves of this pair are shown in Figure 8, aligned for the lag with the largest correlation coefficient (0.891,  $P_1 = 1.7 \times 10^{-3}$ ). GRB 990312 is localized to two sections of a narrow IPN annulus; 020303 is localized to a wide ecliptic latitude band, and the probability of a chance overlap is  $P_2 = 0.41$ . Only the lower spectral indices  $\alpha$  and the fluxes agree, so  $P_3 = 0.949$ . The later burst has 0.96 times the fluence of the earlier one. 990312 displays a sharp dip in its light curve around 2.5 s, which is not present in 020303, but this may be due to intermittent occultation by the spacecraft structure (the spin axis is oriented toward the north ecliptic pole, and the burst is located close to the ecliptic plane). GRB 020303 also displays a dip around 1 s and a peak around 5 s that do not

correspond to 990312, and which also might be explained by occultation and microlensing. The evidence for lensing is weak for this pair. The overlapping localizations for this pair do not overlap with the localization of GRB 960924 above.  $P_j = 6.6 \times 10^{-4}$ .

GRB 19950114\_47434/19950704\_11431. The time delay is 170 days. The light curves of this pair are shown in Figure 9, aligned for the lag with the largest correlation coefficient (0.883,  $P_1 = 0.025$ ). Both bursts are localized to sections of narrow IPN annuli; the probability of a chance overlap is approximately  $P_2 = 0.30$ . Only the spectral indices match;  $E_{\text{peak}}$  differ by over a factor of 2;  $P_3 = 0.949$ . The later burst has 1.9 times the fluence of the earlier one. There are prominent features in 950114 that are missing in 950704, which would require a microlensing explanation to reconcile. The region of intersection is inconsistent with those of the 950114/151021 and 950704/051012 pairs.  $P_j = 7.1 \times 10^{-3}$ .

Note that in the cases where one burst appears in two event pairs (e.g., 19950704/20051012 and 19950114/19950704), this does not imply that the other two bursts (20051012 and 19950114 in this example) will pass the  $r_{\text{max}}$  test; the fact that two time histories are similar does not mean that they are identical. Indeed, all event pairs were tested in this study, and the 20051012/19950114 pair in this example did not pass the test.

## 6. Targeted Searches

The search described above was a blind search through all the burst pairs in the sample. However, a number of bursts

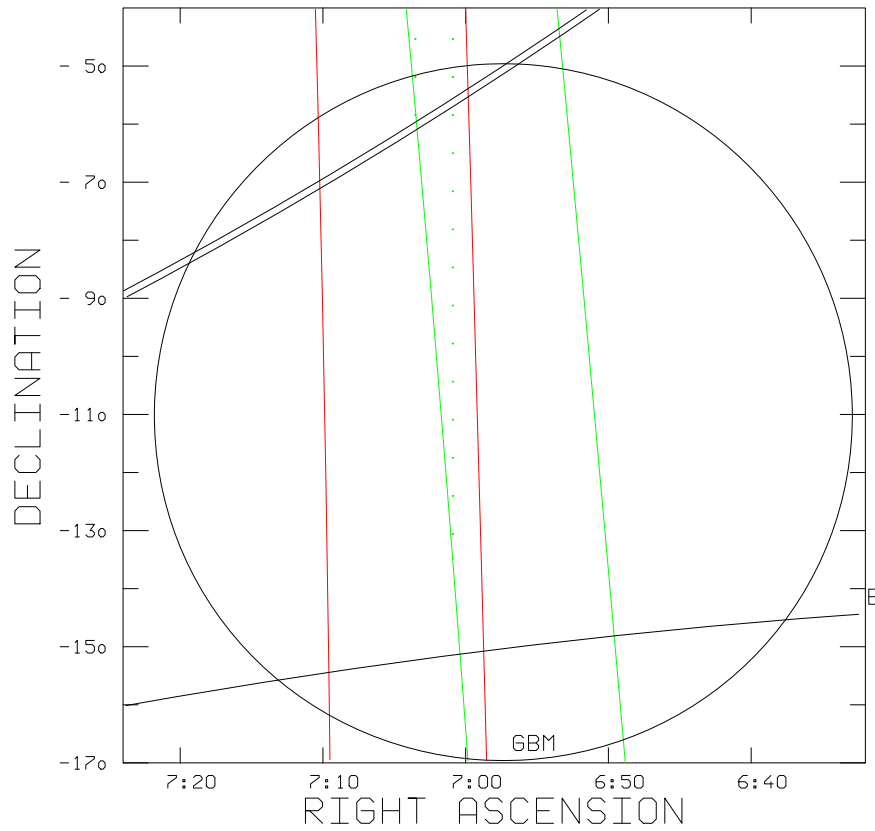


**Figure 10.** Localization information for GRB 19950114\_47434 and GRB 20151021\_68368. GRB 19950114 is localized to an IPN annulus (black line pair) and a *Konus* ecliptic latitude band; one part of the band is represented by the black line marked E. GRB 20151021 is localized to two IPN annuli (green and red line pairs, whose common region is indicated with green dots) and a *Fermi* GBM error circle (black). The circle is an approximation to the  $3\sigma$ , statistical plus systematic error region. The region in common to all the localization information is the section of the 19950114 annulus between the green line on the left and the red line on the right. The probability of a chance overlap between all the localizations is 0.023.

**Table 1**  
Six Candidate Burst Pairs

GRB1/GRB2 year, month, day, seconds	Observed by <sup>a</sup>	Joint Probability $P_j$	Time Delay, $d$	Fluence Ratio Later Burst/ earlier burst	GCN Circular References
19950704_11431/20051012_43209	U,Y,K/K,R,I	$5.9 \times 10^{-6}$	3753	0.45	...
19960924_42119/20020303_82040	U,B,T,K/U,K	$3.3 \times 10^{-6}$	1986	0.093	...
20000821_33589/20041007_07328	U,K/O,K,R,I	$2.1 \times 10^{-5}$	1507	1.7	...
19950114_47434/20151021_68368	U,T,K/K,I,F	$2.4 \times 10^{-5}$	7585	1.1	1
19990312_69909/20020303_82040	U,K/U,K	$6.6 \times 10^{-4}$	1087	0.96	...
19950114_47434/19950704_11431	U,T,K/U,Y,K	$7.1 \times 10^{-3}$	170	1.9	...

**Note.**

<sup>a</sup> Spacecraft abbreviations: B—*Compton Gamma-Ray Observatory BATSE*, F—*Fermi GBM*, I—*INTEGRAL SPI-ACS*, K—*Wind-Konus*, O—*Mars Odyssey*, R—*RHESSI*, T—*Wind TGRS*, U—*Ulysses*, Y—*Yohkoh HXS*.

**Reference.** (1) Veres & Meegan (2015).

warrant a closer look. For over 50 bursts to date, both a source redshift and an intervening redshift have been reported. 11 of them are in the sample; they are given in Table 3. All of them went through the analysis and rejection methods of the previous search and none met the acceptance criteria. However, because these events are prime candidates for lensing, they were subjected to a reanalysis with a lower correlation coefficient threshold. This is justified for two reasons. First, the small number of events means that considerably fewer burst pairs have to be analyzed: 25,300 instead of 2,646,150, making the number of spurious correlations much lower. Second, for

each of the 11 bursts, an optical counterpart was detected, which means that its position is known very accurately and the probability of a chance positional overlap is also considerably reduced. Thus these bursts were examined again with a threshold  $r_{\max} = 0.74$ , corresponding to an empirical probability equivalent to roughly  $2\sigma$ . For the 11 bursts, the resulting number of burst pairs exceeding the threshold ranged between 0 and 542. The localizations of these pairs were then examined to see whether any were consistent with a common origin, and if so, whether they met the trigger criterion. Based on the areas searched, we would have expected 3.6 random coincidences,

**Table 2**  
Time-integrated Energy Spectra of the Six Candidate Burst Pairs (Band Model, 90% Confidence Levels)

GRB	$\alpha$	$\beta$	$E_{\text{peak}}$ , keV	Fluence erg cm <sup>-2</sup> 10 keV–10 MeV	64 ms Peak Flux erg cm <sup>-2</sup> s <sup>-1</sup> 10 keV–10 MeV
19950704_11431	$-0.72^{+0.13}_{-0.09}$	$-3.90^{+1.05}_{-6.10}$	$277^{+32}_{-32}$	$2.51 \times 10^{-5} \pm 2.37 \times 10^{-6}$	$1.82 \times 10^{-5} \pm 1.712 \times 10^{-6}$
20051012_43209	$-0.60^{+0.21}_{-0.18}$	$-2.64^{+0.32}_{-0.71}$	$224^{+32}_{-27}$	$1.13 \times 10^{-5} \pm 2.16 \times 10^{-6}$	$8.60 \times 10^{-6} \pm 1.644 \times 10^{-6}$
19960924_42119	$-0.81^{+0.03}_{-0.03}$	$-3.57^{+0.20}_{-0.28}$	$295^{+7}_{-7}$	$2.77 \times 10^{-4} \pm 4.41 \times 10^{-6}$	$1.59 \times 10^{-4} \pm 2.583 \times 10^{-6}$
20020303_82040	$-0.52^{+0.13}_{-0.12}$	$-4.12^{+0.92}_{-5.88}$	$268^{+17}_{-16}$	$2.58 \times 10^{-5} \pm 2.04 \times 10^{-6}$	$1.60 \times 10^{-5} \pm 1.262 \times 10^{-6}$
20000821_33589	$-0.39^{+0.40}_{-0.39}$	$-2.83^{+0.38}_{-7.18}$	$126^{+30}_{-18}$	$5.51 \times 10^{-6} \pm 1.02 \times 10^{-6}$	$6.91 \times 10^{-6} \pm 1.281 \times 10^{-6}$
20041007_07328	$-0.55^{+0.35}_{-0.22}$	$-3.94^{+2.00}_{-6.06}$	$932^{+357}_{-331}$	$9.41 \times 10^{-6} \pm 4.29 \times 10^{-6}$	$1.03 \times 10^{-5} \pm 4.690 \times 10^{-6}$
19950114_47434	$-0.70^{+0.16}_{-0.12}$	$-3.02^{+0.33}_{-0.74}$	$120^{+9}_{-10}$	$1.32 \times 10^{-5} \pm 1.22 \times 10^{-6}$	$6.81 \times 10^{-6} \pm 6.283 \times 10^{-7}$
20151021_68368	$-0.74^{+0.23}_{-0.16}$	$-2.74^{+0.41}_{-7.26}$	$254^{+41}_{-43}$	$1.44 \times 10^{-5} \pm 2.59 \times 10^{-6}$	$8.09 \times 10^{-6} \pm 1.455 \times 10^{-6}$
19990312_69909	$-0.48^{+0.30}_{-0.26}$	$-2.34^{+0.14}_{-0.21}$	$177^{+28}_{-21}$	$2.68 \times 10^{-5} \pm 3.02 \times 10^{-6}$	$1.29 \times 10^{-5} \pm 1.456 \times 10^{-6}$
20020303_82040	$-0.52^{+0.13}_{-0.12}$	$-4.12^{+0.92}_{-5.88}$	$268^{+17}_{-16}$	$2.58 \times 10^{-5} \pm 2.04 \times 10^{-6}$	$1.60 \times 10^{-5} \pm 1.262 \times 10^{-6}$
19950114_47434	$-0.70^{+0.16}_{-0.12}$	$-3.02^{+0.33}_{-0.74}$	$120^{+9}_{-10}$	$1.32 \times 10^{-5} \pm 1.22 \times 10^{-6}$	$6.81 \times 10^{-6} \pm 6.283 \times 10^{-7}$
19950704_11431	$-0.72^{+0.13}_{-0.09}$	$-3.90^{+1.05}_{-6.10}$	$277^{+32}_{-32}$	$2.51 \times 10^{-5} \pm 2.37 \times 10^{-6}$	$1.82 \times 10^{-5} \pm 1.712 \times 10^{-6}$

**Table 3**  
11 Bursts with Intervening Redshifts

GRB	Reference	$z_{\text{source}}$	$z_{\text{intervening}}$
050820	1	2.6147	2.3597
061007	2	1.261	1.06
071003	3	>.937	0.370, 0.372
080319B	4	0.937	0.530
090812	5	2.452	not specified
111008A	6	4.9898	4.61
120119A	7	1.728	1.212
140419A	8	3.956	2.686
141220A	9	1.3195	1.280, 0.527
150403A	10	2.06	1.76
151021A	11	2.330	1.490

**References.** (1) Ledoux et al. (2005); (2) Osip et al. (2006); (3) Fugazza et al. (2007); (4) Vreeswijk et al. (2008); (5) de Ugarte Postigo et al. (2009); (6) Wiersema et al. (2011); (7) Cucchiara & Prochaska (2012); (8) Tanvir et al. (2014); (9) de Ugarte Postigo et al. (2014); (10) Pugliese et al. (2015); (11) de Ugarte Postigo et al. (2015).

and 2 coincidences were actually found. None met the trigger criterion, and all were rejected without further analysis.

Two other events, GRB 990123 and GRB 000301C, have been proposed as candidates for lensing. It was suggested that the high apparent luminosity of GRB 990123 could be due to magnification (Blandford & Helfand 1999), although this has been questioned (Bloom et al. 1999), while achromatic, short-timescale variability in the afterglow of GRB 000301C could be due to microlensing (Garnavich et al. 2000a). While redshifts have been measured for both events, there is no conclusive evidence for intervening systems. Nevertheless, we have carried out the same reanalysis of these bursts as above. (XRF 060428B has also been suggested as a strongly lensed burst (Perley et al. 2007), but as it was not observed by *Konus*, it was not included in this analysis.) For GRB 990123, 196 events were above the  $r_{\text{max}} = 0.74$  criterion. Based on their areas, 0.08 random spatial coincidences would have been expected, and one was found. It did not meet the trigger criterion. For GRB 000301C, 21 events met the  $r_{\text{max}}$  criterion.

Based on their areas, 0.003 random coincidences would have been expected, and none were found.

## 7. Discussion and Conclusions

We have developed methods to search efficiently through 2,646,150 burst pairs for a trifecta of matching time histories, consistent localizations with low chance coincidence probabilities, and similar energy spectra. We believe this to be the first search that utilizes all the available data for GRBs. We identified six candidate pairs with figures of merit spanning a range of 1200, but none wear the triple crown. Indeed, to date, no bursts have been proposed with high confidence as a lensed pair in any search. The gamma-ray burst literature is replete with discussions about lensing, its signatures, and its effects on GRB studies (Paczynski 1986, 1987; Babul et al. 1987; McBreen & Metcalfe 1988; Blaes & Webster 1992; Blandford & Narayan 1992; Gould 1992; Mao 1992, 1993; Narayan & Wallington 1992; Schneider et al. 1992; McBreen et al. 1993; Nemiroff et al. 1993a, 1993b, 1994a, 1994b, 1998, 2000a, 2000b; Stanek et al. 1993; Wambsganss 1993; Grossman & Nowak 1994; Nowak & Grossman 1994; Beskin 1995; Hanlon et al. 1995; Nemiroff & Gould 1995; Ulmer & Goodman 1995; Ball 1996; Kolb & Tkachev 1996; Marani et al. 1996, 1997, 1998, 1999; Marani & Nemiroff 1996; Williams 1996; Williams & Wijers 1997; Beskin et al. 1998, 1999; Loeb & Perna 1998; Andersen et al. 1999; Blandford & Helfand 1999; Holz et al. 1999; Komberg et al. 1999; Garnavich et al. 2000a, 2000b; Wyithe & Turner 2000; Blandford 2001; Gaudi & Loeb 2001; Gaudi et al. 2001; Granot & Loeb 2001; Ioka & Nakamura 2001; Koopmans & Wambsganss 2001; Mao & Loeb 2001; Panaitescu 2001; Porciani & Madau 2001; Li & Ostriker 2003; Walker & Lewis 2003; Williams & Frey 2003; Baltz & Hui 2005; Pedersen et al. 2005; Hirose et al. 2006; Prochter et al. 2006; Perley et al. 2007; Porciani et al. 2007; Biesiada & Piorowska 2009; Tejos et al. 2009; Vergani et al. 2009; Bagoly & Veres 2010; Veres et al. 2010; Bagoly et al. 2011; Davidson et al. 2011; Wang & Dai 2011; Wyithe et al. 2011; Barnacka et al. 2012; Rapoport et al. 2012, 2013; Zhang et al. 2012; Quimby et al. 2013; Sudilovsky et al. 2013; Petitjean et al. 2016; Christensen et al. 2017; Fan et al. 2017). A bibliography of 88

papers has been extracted from the IPN GRB bibliography<sup>14</sup> and is available online<sup>15</sup> with titles. We have cited them here for completeness. Many of these publications predate the discovery of the cosmological nature of bursts and are no longer directly relevant to the present study. Some studies, which are comparable to the present one, involve searches through the BATSE and *Fermi* data for lensed bursts (Nemiroff et al. 1993a, 1993b, 1994a, 1994b, 2000a; Marani et al. 1996, 1998; Bagoly & Veres 2010; Veres et al. 2010; Davidson et al. 2011). These searches involved up to 1892 BATSE bursts and 515 *Fermi* GBM ones. The results were negative in all cases. The efficiencies of these missions, taking Earth-occultation and duty cycles into account, are roughly 50%, which is less than the present one. On the other hand the greater sensitivities of these experiments would make it possible to detect lensed burst pairs that our search could not, such as two bursts below our threshold, or one above and one below. Quantifying the net effect would strongly depend on assumptions about the apparent luminosities of lensed burst pairs. If the comparison is restricted to searches for bursts in which each of the burst pair is above the threshold of the instrument, we believe that the *Konus*/IPN search described here is the most extensive one to date, considering the number of bursts, the time span, and the efficiency.

The six candidate burst pairs involve relatively simple time histories, which partly explains why they met the  $r_{\max} > 0.88$  test. Although we do not consider any of them to be convincing evidence for lensing, it is interesting to note that the time delays in the seven pairs ranged from 170 to 7585 days. For comparison, the longest delay found in the master lens database (Kochanek et al. 2018) is 822 days, and five out of the six candidates exceed this value, implying, among other things, much larger deflection angles. These could be resolved, in principle, by radio, optical, or X-ray observations of the counterpart, or even by IPN techniques under the best conditions.






We have independently estimated the rate of detection of both images of a gravitationally lensed GRB using the methodology proposed, e.g., in Grossman & Nowak (1994), using the standard  $\Lambda$ CDM cosmological model with parameters  $H_0 = 67.3 \text{ km s}^{-1} \text{ Mpc}^{-1}$ ,  $\Omega_\Lambda = 0.685$ , and  $\Omega_M = 0.315$  (Planck Collaboration et al. 2014). To model the KW GRB population we used the GRB luminosity function and the GRB formation rate from Tsvetkova et al. (2017). As a model of the gravitational lens we used the Singular Isothermal Sphere approximation for the mass distribution, the simplest model for extended lenses (see, e.g., Schneider 2006). Assuming no cosmological evolution of the GRB luminosity function (see Tsvetkova et al. 2017 for details), we estimate the detection rate of both GRB images as  $\approx 0.05$  events per year, i.e.,  $\approx 1$  pair of GRB images during the entire time interval of the present search. Using a GRB luminosity function and formation rate corrected for cosmological evolution, we estimate the detection rate of both GRB images as  $\approx 0.02$  events per year, or  $\approx 0.5$  pair of GRB images during the same time interval. These numbers are roughly consistent with the nondetection of lensed bursts in our study.

Assuming that no lensed pairs were detected, the approximate  $3\sigma$  upper limit to the actual number of lensed bursts is 5.8

for a Poisson distribution. This must be increased by three factors:  $d$ , the duty cycle (0.95),  $s$ , the time delay sensitivity (0.982), and  $a$ , the acceptance rate (0.82). Then if bursts above the *Konus* detection threshold are considered, the optical depth to lensing is  $< 5.8/2301 \text{ dsa}$ , or 0.0033. This rules out the estimates of Wyithe et al. (2011), but is consistent with those of Turner et al. (1984) and Treu (2010) for optical sources. The sensitivity of the present method will increase slowly with time, as *Konus* triggers on about 150 bursts per year. Another, faster possibility is to expand the method to utilize bursts from other spacecraft in addition to those from *Konus*, which would make it sensitive to burst pairs in which one or both events is below the *Konus* threshold, but at the expense of introducing systematic uncertainties inherent in the comparison of light curves from different instruments. Nevertheless, until at least one burst pair is identified with high confidence, the two major hurdles remain first, the uncertainty in the degree to which light curves and energy spectra should agree, and second, the relatively high probability of coincident IPN localizations.

Support for this project came from NASA’s 2014 Astrophysics Data Analysis Program, grant NNX15AE60G. D.S.S., R.L.A., D.D.F., A.A.K., A.V.K., and M.V.U. acknowledge support from RFBF grant 18-02-00062. This research has made use of data, software, and/or web tools obtained from the High Energy Astrophysics Science Archive Research Center (HEASARC), a service of the Astrophysics Science Division at NASA/GSFC and of the Smithsonian Astrophysical Observatory’s High Energy Astrophysics Division. *Mars Odyssey* HEND instrument data processing and analysis were supported by Federal Agency for Scientific Organizations “Exploration” theme grant AAAA-A18-118012290370-6.

## ORCID iDs

K. Hurley  <https://orcid.org/0000-0003-3315-1975>  
 A. E. Tsvetkova  <https://orcid.org/0000-0003-0292-6221>  
 D. S. Svinkin  <https://orcid.org/0000-0002-2208-2196>  
 D. D. Frederiks  <https://orcid.org/0000-0002-1153-6340>  
 A. L. Lysenko  <https://orcid.org/0000-0002-3942-8341>

## References

- Andersen, M., Castro-Tirado, A., Hjorth, J., et al. 1999, *Sci*, **283**, 2075  
 Aptekar, R., Frederiks, D., Golenetskii, S., et al. 1995, *SSRv*, **71**, 265  
 Babul, A., Paczynski, B., & Spergel, D. 1987, *ApJL*, **316**, L49  
 Bagoly, Z., & Veres, P. 2010, in AIP Conf. Proc. 1279, Deciphering the Ancient Universe with Gamma-Ray Bursts, ed. N. Kawai & S. Nagataki (Melville, NY: AIP), 293  
 Bagoly, Z., Veres, P., & Szécsi, D. 2011, in AIP Conf. Proc. 1358, Gamma-Ray Bursts 2010, ed. J. McEnery, J. Racusin, & N. Gehrels (Melville, NY: AIP), 5  
 Ball, J. 1996, in AIP Conf. Proc. 384, Gamma-Ray Bursts: 3rd Huntsville Symposium, ed. C. Kouveliotou, M. Briggs, & G. Fishman (Melville, NY: AIP), 719  
 Baltz, E., & Hui, L. 2005, *ApJ*, **618**, 403  
 Band, D., Matteson, J., Ford, L., et al. 1993, *ApJ*, **413**, 281  
 Barnacka, A., Glöckstein, J.-F., & Moderski, R. 2012, *PhRvD*, **86**, 043001  
 Beskin, G. 1995, in Flares and Flashes, ed. J. Greiner, H. Duerbeck, & R. Gershberg (Berlin: Springer), 363  
 Beskin, G., Shearer, A., Golden, A., et al. 1999, *A&AS*, **138**, 587  
 Beskin, G., Shearer, A., Redfern, A., et al. 1998, *NuPhB*, **69**, 703  
 Biesiada, M., & Piorowska, A. 2009, *MNRAS*, **396**, 946  
 Blaes, O., & Webster, R. 1992, *ApJL*, **391**, L63  
 Blandford, R. 2001, *PASP*, **113**, 1309  
 Blandford, R., & Helfand, D. 1999, *MNRAS*, **305**, L45  
 Blandford, R., & Narayan, R. 1992, *ARA&A*, **30**, 311  
 Bloom, J., Odewahn, C., Djorgovski, S., et al. 1999, *ApJL*, **518**, L1

<sup>14</sup> <http://www.ssl.berkeley.edu/ipn3/biblioweb.pdf>

<sup>15</sup> [http://www.ssl.berkeley.edu/ipn3/gravitational\\_lensing.pdf](http://www.ssl.berkeley.edu/ipn3/gravitational_lensing.pdf)

- Christensen, L., Vergani, S., Schulze, S., et al. 2017, *A&A*, **608**, A84
- Cucchiara, A., Levan, A., Fox, D., et al. 2011, *ApJ*, **736**, 7
- Cucchiara, A., & Prochaska, J. 2012, GCN Circ., 12865, <https://gcn.gsfc.nasa.gov/gcn3/12865.gcn3>
- Davidson, R., Bhat, P. N., & Li, G. 2011, in AIP Conf. Proc. 1358, Gamma-Ray Bursts 2010, ed. J. McEnery, J. Racusin, & N. Gehrels (Melville, NY: AIP), 17
- de Ugarte Postigo, A., Gorosabel, J., Fynbo, J., Wiersema, K., & Tanvir, N. 2009, GCN Circ., 9771, <https://gcn.gsfc.nasa.gov/gcn3/9771.gcn3>
- de Ugarte Postigo, A., Malesani, D., & Xu, D. 2015, GCN Circ., 18426, <https://gcn.gsfc.nasa.gov/gcn3/18426.gcn3>
- de Ugarte Postigo, A., Thoene, C., Gorosabel, J., et al. 2014, GCN Circ., 17198, <https://gcn.gsfc.nasa.gov/gcn3/17198.gcn3>
- Fan, X.-L., Liao, K., Biesiada, M., Piorowska-Kurpas, A., & Zhu, Z.-H. 2017, *PhRvL*, **118**, 091102
- Fugazza, D., Fiore, F., D'Elia, V., et al. 2007, GCN Circ., 6851, <https://gcn.gsfc.nasa.gov/gcn3/6851.gcn3>
- Gamavich, P., Loeb, A., & Stanek, K. 2000a, *ApJL*, **544**, L11
- Gamavich, P., Loeb, A., & Stanek, K. 2000b, *BAAS*, **32**, 1519
- Gaudi, B., Granot, J., & Loeb, A. 2001, *ApJ*, **561**, 178
- Gaudi, B. S., & Loeb, A. 2001, *ApJ*, **558**, 643
- Gould, A. 1992, *ApJL*, **386**, L5
- Granot, J., & Loeb, A. 2001, *ApJL*, **551**, L63
- Grossman, S., & Nowak, M. 1994, *ApJ*, **435**, 548
- Hanlon, L., Hermsen, W., Kippen, R., et al. 1995, *A&A*, **296**, L41
- Hirose, Y., Umemura, M., Yonehara, A., & Sato, J. 2006, *ApJ*, **650**, 252
- Holz, D., Miller, M. C., & Quashnock, J. 1999, *ApJ*, **510**, 54
- Ioka, K., & Nakamura, T. 2001, *ApJ*, **561**, 703
- Kawai, N., Yamada, T., Kosugi, G., Hattori, T., & Aoki, K. 2005, GCN Circ., 3937, <https://gcn.gsfc.nasa.gov/gcn3/3937.gcn3>
- Kochanek, C., Falco, E., Impey, C., et al. 2018, The Gravitational Lens Database, (CASTLES Survey), <http://admin.masterlens.org/lensing.php?>
- Kolb, E., & Tkachev, I. 1996, *ApJL*, **460**, L25
- Komberg, B., Kurt, V., & Kuznetsov, A. 1999, *ARep*, **43**, 580
- Koopmans, L., & Wambsganss, J. 2001, *MNRAS*, **325**, 1317
- Ledoux, C., Vreeswijk, P., Ellison, S., et al. 2005, GCN Circ., 3860
- Li, L.-X., & Ostriker, J. 2003, *ApJ*, **595**, 603
- Loeb, A., & Perna, R. 1998, *ApJ*, **495**, 597
- Mao, S. 1992, *ApJL*, **389**, L41
- Mao, S. 1993, *ApJ*, **402**, 382
- Mao, S., & Loeb, A. 2001, *ApJL*, **547**, L97
- Marani, G., & Nemiroff, R. 1996, in ASP Conf. Ser. 88, Clusters, Lensing, and the Future of the Universe, ed. V. Trimble & A. Reisenegger, 107
- Marani, G., Nemiroff, R., Norris, J., & Bonnell, J. 1996, in AIP Conf. Proc. 384, Gamma-Ray Bursts: 3rd Huntsville Symposium, ed. C. Kouveliotou, M. Briggs, & G. Fishman (Melville, NY: AIP), 487
- Marani, G., Nemiroff, R., Norris, J., Hurley, K., & Bonnell, J. 1997, *BAAS*, **29**, D69
- Marani, G., Nemiroff, R., Norris, J., Hurley, K., & Bonnell, J. 1998, in AIP Conf. Proc. 428, Fourth Huntsville Gamma-Ray Burst Symposium, ed. C. Meegan, R. Preece, & T. Koshut (Melville, NY: AIP), 166
- Marani, G., Nemiroff, R., Norris, J., Hurley, K., & Bonnell, J. 1999, *ApJL*, **512**, L13
- McBreen, B., & Metcalfe, L. 1988, *Natur*, **332**, 234
- McBreen, B., Plunkett, S., & Metcalfe, L. 1993, *A&AS*, **97**, 81
- Narayan, R., & Wallington, S. 1992, *ApJ*, **399**, 368
- Nemiroff, R., & Gould, A. 1995, *ApJL*, **452**, L111
- Nemiroff, R., Horack, J., Norris, J., et al. 1993a, in AIP Conf. Proc. 280, Compton Gamma-Ray Observatory, ed. M. Friedlander, N. Gehrels, & D. Macomb (Melville, NY: AIP), 974
- Nemiroff, R., Marani, G., Norris, J., et al. 2000a, in AIP Conf. Proc. 526, Gamma-Ray Bursts: 5th Huntsville Symposium, ed. R. M. Kippen, R. S. Mallozzi, & G. J. Fishman (Melville, NY: AIP), 663
- Nemiroff, R., Marani, G., Norris, J., & Bonnell, J. 2000b, *BAAS*, **32**, 1519
- Nemiroff, R., Norris, J., Bonnell, J., & Marani, G. 1998, *ApJL*, **494**, L173
- Nemiroff, R., Norris, J., Wickramasinghe, W., et al. 1993b, *ApJ*, **414**, 36
- Nemiroff, R., Wickramasinghe, W., Norris, J., et al. 1994a, *ApJ*, **432**, 478
- Nemiroff, R., Wickramasinghe, W., Norris, J., et al. 1994b, in AIP Conf. Proc. 307, Gamma-Ray Bursts: 2nd Workshop, ed. G. Fishman, J. Brainerd, & K. Hurley (Melville, NY: AIP), 150
- Nowak, M., & Grossman, S. 1994, *ApJ*, **435**, 557
- Osip, D., Chen, H.-W., & Prochaska, J. 2006, GCN Circ., 5715, <https://gcn.gsfc.nasa.gov/gcn3/5715.gcn3>
- Paczynski, B. 1986, *ApJL*, **308**, L43
- Paczynski, B. 1987, *ApJL*, **317**, L51
- Panaiteanu, A. 2001, *ApJ*, **556**, 1002
- Pedersen, K., Eliasdottir, A., Hjorth, J., et al. 2005, *ApJL*, **634**, L17
- Perley, D., Bloom, J., Butler, N., Li, W., & Chen, H.-W. 2007, in AIP Conf. Proc. 937, Supernova 1987A: 20 Years After: Supernovae and Gamma-Ray Bursters, ed. S. Immler & K. Weiler (Melville, NY: AIP), 526
- Petitjean, P., Wang, F., Wu, X., & Wei, J. 2016, *SSRv*, **202**, 195
- Planck Collaboration, Ade, P. A. R., Aghanim, N., et al. 2014, *A&A*, **571**, A16
- Porciani, C., & Madau, P. 2001, *ApJ*, **548**, 522
- Porciani, C., Viel, M., & Lilly, S. 2007, *ApJ*, **659**, 218
- Prochter, G., Prochaska, J., Chen, H., et al. 2006, *ApJL*, **648**, L93
- Pugliese, V., Xu, D., Tanvir, N., et al. 2015, GCN Circ., 17672, <https://gcn.gsfc.nasa.gov/gcn3/17672.gcn3>
- Quimby, R., Werner, M., Oguri, M., et al. 2013, *ApJL*, **768**, L20
- Rapoport, S., Onken, C., Schmidt, B., et al. 2012, *ApJ*, **754**, 139
- Rapoport, S., Onken, C., Wyithe, J. S., Schmidt, B., & Thygesen, A. 2013, *ApJ*, **766**, 23
- Schneider, P. 2006, in Gravitational Lensing: Strong, Weak and Micro, ed. G. Meylan, P. Jetzer, & P. North (Berlin: Springer), 1
- Schneider, P., Ehlers, J., & Falco, E. 1992, Gravitational Lenses (New York: Springer)
- Stanek, K., Paczynski, B., & Goodman, J. 1993, *ApJL*, **413**, L7
- Sudilovsky, V., Greiner, J., Rau, A., et al. 2013, *A&A*, **662**, A143
- Svinkin, D., Frederiks, D., Aptekar, R., et al. 2016, *ApJS*, **224**, 10
- Tanvir, N., Levan, A., Cucchiara, A., et al. 2014, GCN Circ., 16125, <https://gcn.gsfc.nasa.gov/gcn3/16125.gcn3>
- Tejos, N., Lopez, S., Prochaska, J., et al. 2009, *ApJ*, **706**, 1309
- Tinney, C., Stathakis, R., Cannon, R., & Galama, T. 1998, *IAUC*, 6896, <http://www.cbat.eps.harvard.edu/iauc/06800/06896.html>
- Treu, T. 2010, *ARA&A*, **48**, 87
- Tsvetkova, A., Frederiks, D., Golenetskii, S., et al. 2017, *ApJ*, **850**, 161
- Turner, E., Ostriker, J., & Gott, J. R., III 1984, *ApJ*, **284**, 1
- Ulmer, A., & Goodman, J. 1995, *ApJ*, **442**, 67
- Veres, P., Bagoly, Z., Horvath, I., Meszaros, A., & Balazs, L. 2010, in Stanford eConf C0911022, ed. W. N. Johnson & D. J. Thompson, <http://www.slac.stanford.edu/econf/C0911022/>
- Veres, P., & Meegan, C. 2015, GCN Circ., 18434, <https://gcn.gsfc.nasa.gov/gcn3/18434.gcn3>
- Vergani, S., Petitjean, P., Ledoux, C., et al. 2009, *A&A*, **503**, 771
- Vreeswijk, P., Smette, A., Malesani, D., et al. 2008, GCN Circ., 7444, <https://gcn.gsfc.nasa.gov/gcn3/7444.gcn3>
- Walker, M., & Lewis, G. 2003, *ApJ*, **589**, 844
- Wambsganss, J. 1993, *ApJ*, **406**, 29
- Wang, F.-Y., & Dai, Z. G. 2011, *A&A*, **536**, A96
- Wiersema, K., Flores, H., D'Elia, V., et al. 2011, GCN Circ., 12431, <https://gcn.gsfc.nasa.gov/gcn3/12431.gcn3>
- Williams, L. 1996, *ApJ*, **472**, 497
- Williams, L., & Frey, N. 2003, *ApJ*, **583**, 594
- Williams, L., & Wijers, R. 1997, *MNRAS*, **286**, L11
- Wyithe, J., Oh, S., & Pindor, B. 2011, *MNRAS*, **414**, 209
- Wyithe, J., & Turner, E. 2000, *MNRAS*, **319**, 1163
- Zhang, B.-B., Burrows, D., Zhang, B., et al. 2012, *ApJ*, **748**, 132